HIGH-TEMPERATURE HEAT PUMPS FOR GEOTHERMAL APPLICATIONS IN AFRICA: THERMODYNAMIC, ECONOMIC AND ENVIRONMENTAL EVALUATION.

Zuffi Claudio[1]*, Ramundi Filippo[1], Fiaschi Daniele[1]

[1]University of Florence, Department of Industrial Engineering, Florence, Italy

*Corresponding Author: claudio.zuffi@unifi.it

ABSTRACT

Low- and high-enthalpy geothermal resources are ubiquitously distributed across the African continent, yet their utilization remains constrained. The Rift Valley region stands out as a focal point, showcasing myriad high-enthalpy manifestations of geothermal resources, and therefore for the production of electricity. Meanwhile, the mainland is characterized by an abundance of medium- and low-enthalpy resources and a thorough analysis of this potential is necessary for the sustainable development of the continent. Notably, geothermal resources harbor substantial energy potential that lends itself well to a diverse range of applications. The subject of investigation in this study revolves around the implementation of a high-temperature heat pump (HTHP) that exploits geothermal resources. Specifically, two distinct cases are evaluated: a one-level pressure system and a two-level pressure system. The primary objective of this research is to formulate a comprehensive model capable of predicting the thermodynamic efficiencies, economic costs, and environmental impacts associated with HTHPs. This endeavor entails the development of metamodels designed to forecast the dimensions of the HTHP, including its installed kilowatt capacity and its heat output. Additionally, the model assesses the levelized cost of heat (LCOH). Furthermore, the potential environmental footprint of the HTHP is estimated through the evaluation of its carbon dioxide equivalent emissions via a Life Cycle Assessment. This latter step is executed by employing a parametric Life Cycle Inventory (pLCI), establishing a link between the environmental impact of HTHP construction and the thermodynamic model. To validate the model and delineate potential applications, a series of case studies are examined, specifically focusing on various African regions. The central finding of this study underscores that the low-enthalpy geothermal resources available in Africa have the potential to yield substantial energy savings and significant environmental benefits. These findings are pivotal in fostering sustainable development within the region, marking geothermal energy as a fundamental contributor to the broader sustainability goals.

1 INTRODUCTION

The African continent is endowed with significant geothermal potential, particularly concentrated in the eastern and southern regions, aligned with the East African Rift System (EARS) (Elbarbary et al. 2022). This geological phenomenon presents a promising avenue for the utilization of geothermal energy resources, due to the correlation between geothermal activity and Quaternary volcanism along the rift axis (Enerdata, 2013; ESY,2019). Moreover, Kenya's Rift Valley stands out as a hotspot for geothermal exploration and exploitation, boasting vast reserves estimated at 10,000 MW spread across 14 sites (Waruru, 2016; ERC, 2012; KME, 2018). While conventional geothermal power plants have historically focused on high enthalpy resources, recent advancements have shed light on the untapped potential of medium to low enthalpy resources (Stober & Bucher, 2013; Chandrasekharam & Bundschuh, 2008). Notably, the adoption of cascading approaches, leveraging different temperature levels of geothermal energy, emerges as a promising strategy to maximize resource utilization efficiency (Jin et al., 2007; Rubio-Maya et al., 2015; Budiarto et al., 2014). The direct utilization of geothermal energy is the oldest and most versatile way to harness geothermal energy of medium and low enthalpy. Current trending direct uses are mainly for heating systems working directly or through heat pumps, aquaculture, drying crops, growing plants and vegetables in greenhouses, processes of the

https://doi.org/10.52202/077185-0136

paper and the cement industry, food processing, brewing, dyeing of fabrics, snow melting, cooling spaces and balneology, among others (Lund et al. 2011-2016). In this context, Africa stands at the forefront of harnessing geothermal energy for sustainable development, (Waruru, 2016). This underscores the continent's commitment to transitioning towards cleaner and more reliable energy sources to meet growing energy demands while mitigating environmental impacts (Rubio-Maya et al. 2015). Integration of High Temperature Heat Pump (HTHP) with geothermal systems offers potential energy consumption benefits (Arpagaus et al. 2018). Despite being underutilized, geothermal energy presents challenges due to the need for specific extraction locations (Arpagaus et al. 2018) The economic and Environmental feasibility of these methods is a key consideration for future studies. The objective of this paper is to provide a comprehensive model for the sustainability assessment of HTHP applied for geothermal energy and apply it to a case study of the Malawi geothermal resource. This work was carried out as part of the European Long-Term Joint European Union-African Union Research and Innovation Partnership on Renewable Energy, Geothermal Atlas for Africa (LEAP-RE GAA 2020) project.

2 METHODOLOGIES

The methodology section of this study delineates the comparative analysis of two distinct system configurations of High-Temperature Heat Pumps (HTHP) as illustrated in Figure 1. Cycle A operates at a singular pressure level, incorporating an evaporator, a compressor, a condenser, and an expansion valve. Conversely, Cycle B is characterized by a dual pressure level system, in which a separator is integrated. This separator works at an intermediate pressure, situated between the cycle's minimum and maximum pressures. Its role is crucial in recovering some of the heat from the working fluid after condensation, as well as decreasing the compressor workload, thus increasing the system's coefficient of performance (COP). The systems configurations for both cycles are derived from existing literature (Cao et al., 2014) employing R152 as working fluid. Initial model validations were conducted using the same fluid; however, This investigation, however, broadens its scope to include environmental considerations by selecting alternative low Global Warming Potential (GWP) fluids, specifically R1233zd(E) and R1234ze(Z) (HFO fluids). The adoption of HFO fluids allows to increase the condenser's temperature compared to R152, thereby raising the user temperature while maintaining the cycle's subcritical condition. The objective of these models is to evaluate the performance of the two cycles, focusing on variables such as the thermal power of the evaporator (Q_{evap}), the heat absorbed by the evaporator from geothermal fluid, the condenser's heat output (Q_{cond}) indicating the system's useful power, the compressor's work requirement (W_{comp}), the COP, the system's working fluid flow rate (m_{cycle}), the generated hot water flow rate (m_{w_out}), and temperature (T_{w_out}).

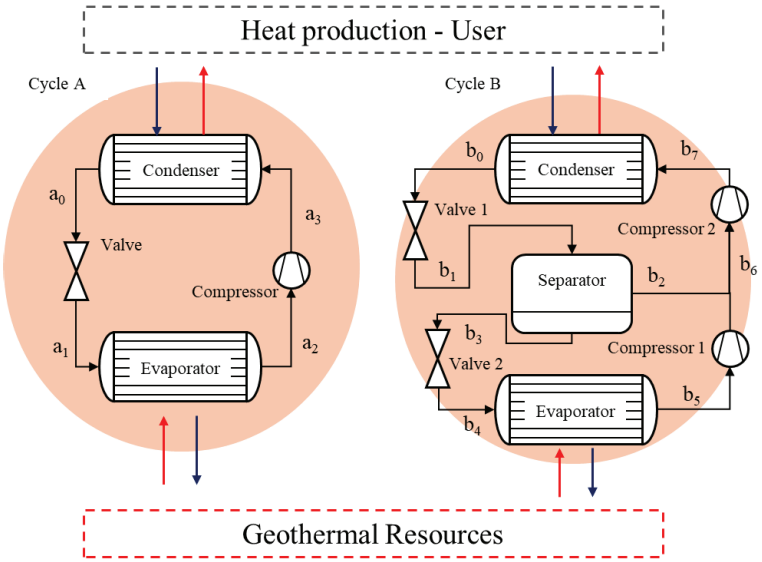

Figure 1: Plant layout of the two cycles: A on the left, B on the right.

https://doi.org/10.52202/077185-0136

After identifying and optimizing these cycle parameters, the study aims to transform the thermodynamic model into a metamodel or surrogate model. This involves defining the inputs, namely the geothermal resource's temperature (T_{geo}) and mass flow rate (m_{geo}), along with their respective variation ranges. T_{geo} is specified to range from 50-100°C, and m_{geo} varies from 1-50 kg/s. To ensure a uniform input distribution, a fixed number of intervals (n_p), set at 25, is established, resulting in an n_p *x* n_p matrix. The validated models are then assessed across n_p *x* n_p input points to generate an output matrix encompassing mechanical component sizes (kW), basic cycle parameters (pressure, temperature, flow rate, etc.), component costs ($), thermo-economic efficiency ($/kWh), and environmental indicators (kg CO_2 eq/kWh). Through multidimensional interpolation, the input matrix is associated with the output matrix to estimate a correlation. This process leads to the creation of a metamodel, which is essentially a function that calculates the HTHP system without requiring direct use of the equations of the underlying model. Furthermore, the application scope of this methodology scenarios involving either surface geothermal water or resource extraction from shallow wells. It's critical to note that the thermodynamic metamodel's efficacy is independent of well depth. However, the model's thermo-economic and environmental impact are significantly influenced by the presence and depth of geothermal wells, as evidenced in recent studies (Shamoushaki et al., 2021; Zuffi et al., 2022). Accordingly, this study engages on a comprehensive thermo-economic and environmental analysis across three scenarios: surface geothermal water extraction ($well_{00}$), extraction from a 500 m well coupled with reinjection into a 300 m well ($well_{500}$), and extraction from a 1000 m well with reinjection into a 600 m well ($well_{1000}$).

2.1 Thermodynamic modeling

In the simplest plant configuration, denoted as Cycle A operating at a single pressure level, the geothermal fluid is introduced into the evaporator. Here, it transfers heat to the working fluid, which flows in counter current. The temperature of the geothermal fluid exiting the evaporator ($T_{geo,out}$) and the specifications of two temperature differentials in the heat exchanger inlet ($\Delta T_{evap,in}$) and outlet ($\Delta T_{evap,out}$) are fixed. Consequently, the temperature of the working fluid at the evaporator inlet is $T_{geo,out}$ - $\Delta T_{evap,in}$, and $T_{geo,in}$ + $\Delta T_{evap,out}$ at the outlet. This dependency on the geothermal well is evident. The working fluid, existing either as saturated steam (x=1) or superheated steam, enters the compressor, tasked with elevating the fluid pressure to match that of the condenser. The condenser's outlet pressure (x=0) and temperature (T_{cond}) are directly determined. Two distinct conditions are examined for the working fluids: the first with Low Temperature (LT) T_{cond} set at 105°C, and the second at High Temperature (HT), evaluating higher temperatures for the two HFO fluids with T_{cond} set at 140°C. Assuming water is drawn at 50°C ($T_{w,in}$) from various sources such as residential, commercial, or industrial applications, it is raised to T_{cond}-$\Delta T_{cond,out}$. Utilizing the heat output provided by the condenser, the flow rate of hot water producible at this temperature is computed. Finally, the expansion valve serves to revert the fluid to evaporator pressure, thereby completing the cycle. In configuration (B), a separator is integrated into the cycle. Following the initial expansion undergone by the fluid in the high-pressure expansion valve, the separator segregates saturated liquid from saturated vapor. The former undergoes further expansion in a second expansion valve until it reaches the evaporator pressure. Meanwhile, the latter is blended with the fluid exiting the low-pressure compressor. This mixture is subsequently pressurized to match the condenser pressure by the high-pressure compressor. Table 1 reports the main parameter for both cycles.

Table 1: Main thermodynamic parameter for the cycles

PARAMETERS		Value	Unit
GEOTHERMAL FLUID OUTLET TEMPERATURE OF	$T_{geo,out}$	45	°C
Evaporator inlet temperature difference	$\Delta T_{evap,in}$	5	°C
Evaporator outlet temperature difference	$\Delta T_{evap,out}$	9	°C
Compressor isentropic efficiency	η_{comp}	0.8	
Inlet temperature of the supplied water	$T_{w,in}$	50	°C
Temperature difference between critical point and condenser	ΔT_{cond}	10	°C
Subcooled temperature in the condenser	ΔT_{sub}	5	°C
Condenser outlet temperature difference	$\Delta T_{cond,out}$	5	°C

https://doi.org/10.52202/077185-0136

Separator pressure difference	ΔP_{sep}	2	bar

The final output of the metamodel is a surface which depends on the two inputs (T_{geo}, m_{geo}) and expresses a thermodynamic parameter of the cycle. For better understanding, the metamodel derived from linear multidimensional interpolation is illustrated in Figure 2, with Cycle A featuring fluid R1233zd(E) as an example.

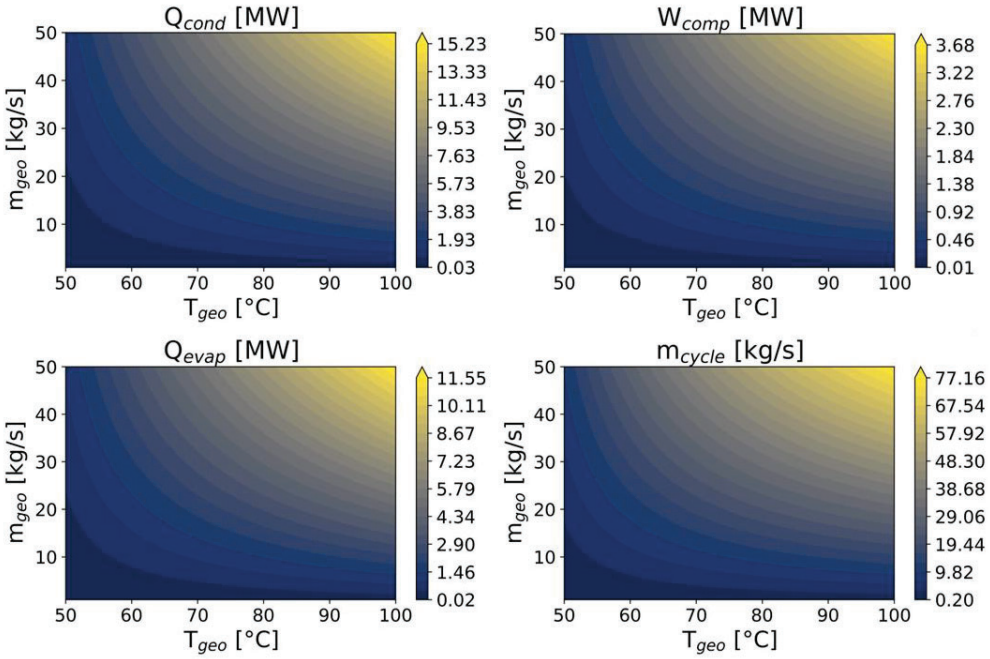

Figure 2: Cycle_a fluid R1233zd(E)

2.2 Thermo-Economic modeling

The economic evaluation comprises two stages. Firstly, the cost analysis of individual plant components is conducted using thermo-economic correlations established by Turton (2008). Secondly, the initial investment cost and the total operating and maintenance cost are assessed to determine the Levelized Cost of Heating (LCOH). The thermodynamic analysis provides fundamental parameters required for thermo-economic correlations, including the surface area needed for heat transfer in the condenser and evaporator, compressor and valve handling flow rates, and separator volume flow rate. For the separator, present in the Cycle B only, the thermo-economic correlation referenced from Mosaffa et al. (2017) is adopted. Table 2 outlines the component types and equations used for each one. Various economic equations exist for geothermal wells, often following linear correlations. In this study, the correlation proposed by Shamoushaki et al., (2021) is adopted. LCOH is a techno-economic parameter crucial for feasibility assessment, enabling the comparison of thermal systems. It quantifies the cost of thermal energy produced per kilowatt-hour ($/kWh), as discussed by de Simón-Martín et al. (2022).

$$LCOH = \frac{C_{TCI} + \sum_{i=1}^{n} \frac{C_{O\&M}}{(1+r)^i}}{\sum_{i=1}^{n} \frac{E_i}{(1+r)^i}} \quad (1)$$

The parameters in equation (1) are: C_{TCI} is the total capital investment cost, $C_{O\&M}$ is the annual operating and maintenance cost, E_i is the annual thermal energy produced, r is the discount rate and n is the lifetime of the energy system. For the calculation of C_{TCI}, the method and parameters used in this work

https://doi.org/10.52202/077185-0136

were taken from Karimi & Mansouri, (2018) and Shamoushaki et al., (2022) and readapted to the case of HTHP, as shown in Table 2. On the other hand, the yearly O&M cost was taken from Beckers et al., (2021) for the general part. On the other hand, the cost of electricity, set at \$0.15/kWh and the total energy consumed by the compressors are taken from the above discussed thermodynamic metamodels . Furthermore, a 7% discount rate and a useful life of 25 years were assumed.

Table 2: Main equations for the thermo-economic model

Cost	Correlation	
Evaporator, Condenser, Compressor	$CP_0 = 10^{K_1+K_2*log_{10}S+K_3*log_{10}S^2}$ $F_P = 10^{C_1+C_2*log_{10}P+C_3*log_{10}P^2}$ $C_{BM} = CP_0 * (B_1 + B_2 * F_M * F_P)$	All variables are indicated in the tables of *Turton 2008*
Valve	$C_{valve} = 114.5 * m_{cycle}$	*M*ossafa et al. 2016
Separator	$C_{sep} = 280.3 * m_{cycle}^{0.67}$	*M*ossafa et al. 2016
Wells	$C_{well} = 2500 * m_{drilled}$	*S*hamoushaki et al. 2021
Total Cost of equipment and wells	$T_{EW} = \sum_{i}^{nc} C_i + C_{well}$	C_i *cost of single component* C_{well} *cost of the wells*
Total Direct Permanent Investment	$C_{DPI} = T_{EW} + C_{site} + C_{serv}$	C_{site} *cost of site preparation* C_{serv} *cost of service facilities*
Total Depreciable Capital	$C_{TDC} = C_{DPI} + C_{cont}$	C_{cont} *cost of contingencies*
Cost Total Permanent Investment	$C_{TPI} = C_{TDC} + C_{land} + C_{royal} + C_{startup}$	C_{royal} *cost of royalties* C_{land} *cost of land* $C_{startup}$ *cost of plant startup*
Total Capital Investment	$C_{TCI} = C_{TPI} + C_{WC}$	C_{WC} *cost of working capital*

2.3 Environmental modeling

The environmental modeling approach adhered to the Life Cycle Assessment (LCA) methodology outlined by ISO 14040 and ISO 14044 standards (ISO, 2021a; ISO, 2021b). The approach used is cradle-to-gate, so the system boundaries include the production and reinjection geothermal wells (if present), the piping system, the surface plant, and the utilization phase. The functional unit for the analysis is the thermal kWh produced by the system. Specifically, to facilitate assessment across numerous scenarios, emphasis was placed on developing a Parametric Life Cycle Inventory (pLCI). pLCI links material and energy consumption throughout the production, operation, maintenance of the HTHP system with its size, as determined by the thermodynamic metamodel. For the construction phase of the system, primary data was collected from commercially available HTHP models sourced from TRANE (2022). A correlation was established between system thermal power (kW) and total weight, as depicted in Figure 3, based on the collected data. Subsequently, the production process for process - *heat pump production, brine-water, 10kW (heat pump, brine-water, 10kW* - from the Ecoinvent database was selected as a reference model. Inputs and outputs of this process were categorized into materials and energy utilized during construction. Percentages for each material and energy consumption were determined, with energy normalized to the total mass of the element. This allows the creation of a new environmental model for the HTHP, incorporating adjusted input and output values multiplied by the correlation obtained in Figure 3. The modeling of geothermal wells was approached linearly, utilizing a shallow well drilling process as described by Karlsdottir et al. (2015). The operation phase accounted for electricity consumption using a reference process for electricity production (*market for electricity, medium voltage | electricity, medium voltage, KE*) while maintenance was evaluated as a 20% material replenishment throughout the life cycle. For analysis, the Ecoinvent 3.7.1 library and the Brightway software, integrated with activity-browser software via Python, were employed. The environmental impact assessed primarily focused on the Climate Change (CC) indicator, expressed through the Environmental Footprint 3.1 methodology.

https://doi.org/10.52202/077185-0136

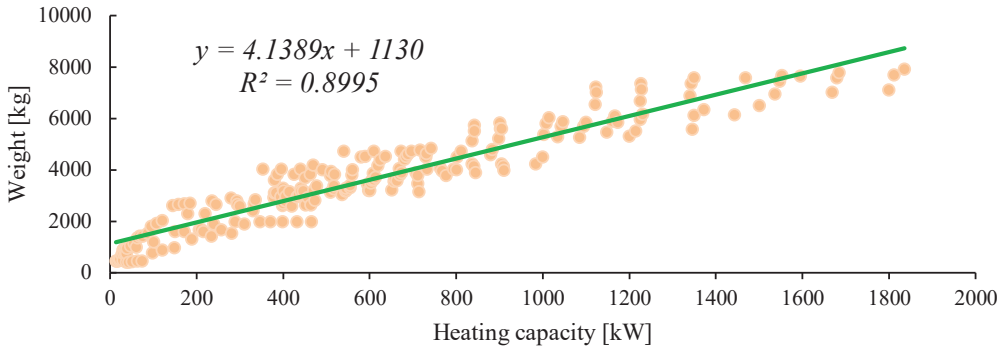

Figure 3: Development of correlation between total system weight and heating capacity

3 CASE STUDIES: MALAWI HOT SPRINGS

The case study evaluated in this paper is the Malawi hot springs. Davalos et al., 2021 performed an extensive study on the geochemical characteristics of 27 hot springs in Malawi, distributed along north to south of the Malawi Rift Zone. In addition to characteristics related to the chemistry of the geothermal resource, the surface temperature assessment is carried out by reporting the temperature of all 27 sites. The surface temperature ranges between 35-80°C, but only hot springs with a temperature above 50°C are taken into consideration in this work, as reported in Table 3.
Unfortunately, the required mass flow rate are not available, for this reason, three flow rate scenarios are defined - High 50 kg/s (Hm), Medium 20 kg/s (Mm), Low 8 kg/s (Lm).

Table 3: Hot spring geothermal sites in Malawai (Davalos et al. 2021)

Hot spring	Surface T°C	Hot spring	Surface T°C
Ngala	54.90	Chombo	66.84
Chiweta	79.70	Madzimawira	63.73
Mphizi Stream	78.70	Ling'ona	58.08
Mtondolo	64.77	Chikwizi	52.17
Mtondolo 2	72.90	July Borehole	51.35
Chiwe	74.90		

Final applications have been defined for possible users of the heat produced at the respective temperatures. In particular, 2 possible uses were chosen:

- Cooking station (CS) supplying steam at 140 °C (HT condition) for cooking food, which requires about 2.89 GWh/year heat load for a group of 5'000 people, (CS_{5k}); 5.79 GWh/year for 10'000 people (CS_{10k}); 29.00 MWh/year for 50'000 people (CS_{50k}) (Kajumba et al. 2022).
- Cassava drying (CD) supplying steam at 100°C (LT condition) for drying vegetables. This process requires about 306 kWh/(ton), so three scenarios are assumed in which a company produces about 10 k tonnes/year CD_{10}, 50 k tonnes/year CD_{50}, and 100 k tonnes/year CD_{100} (Nwakuba et al. 2016).

4 RESULTS

4.1 Parametric analysis

From the analysis conducted on the performance of the system depicted in Figure 4, the COP in all scenarios within Cycle A and Cycle B are compared with previously mentioned fluids. COP is not dependent of m_{geo} and is solely reliant on T_{geo}, as the m_{cycle} increases and decreases at the same rate as

https://doi.org/10.52202/077185-0136

m_{geo}, thus the COP value does not change at variable m_{geo}. The general trend is increasing because, as T_{geo} increases, the difference between high- and low-pressure decreases, so the compressor work is reduced and the COP increases. Focusing on the case of LT, the comparison between Cycle A and Cycle B, the COP for HFO fluids ranges between 3.67 and 4.14 for Cycle A and between 3.53 and 4.13 for Cycle B. Despite the difference in pressure levels for this case, there is no remarkable difference between the two cycles at the thermodynamic level. Conversely, the notable performance difference of fluid R152, exhibiting consistently lower COP across all T_{geo} values, is highlighted. Considering that HFO's environmental performance is better than R152 due to its lower GWP and the better thermodynamic performance of the cycle, the selection of HFO fluids is advised. In addition, with HFO fluids it is possible to maintain the subcritical cycle by increasing the output temperature, in the case of HT. The comparative analysis between Cycle A and Cycle B unveils a notable downturn in COP for both cycles when juxtaposed with the LT scenario. Comparing LT and HP, the cycle A COP experiences a precipitous decline from 1.90 to 2.47, whereas in Cycle B, albeit exhibiting a decrease compared to the preceding scenario, COP ranges between 2.59 and 2.89. The rise of T_{cond} precipitates a growth of pressure consequently augmenting the workload for the compressor. While this yields steam of higher temperature for the end user, it concurrently diminishes the COP of the cycle. This behavior is enhanced in Cycle A, exerting a lower impact on Cycle B due to the presence of two compression levels, which mitigates the overall work required during the compression stage. For the following analyses, Cycle A for the LT scenario and Cycle B for the HT scenario are taken as references.

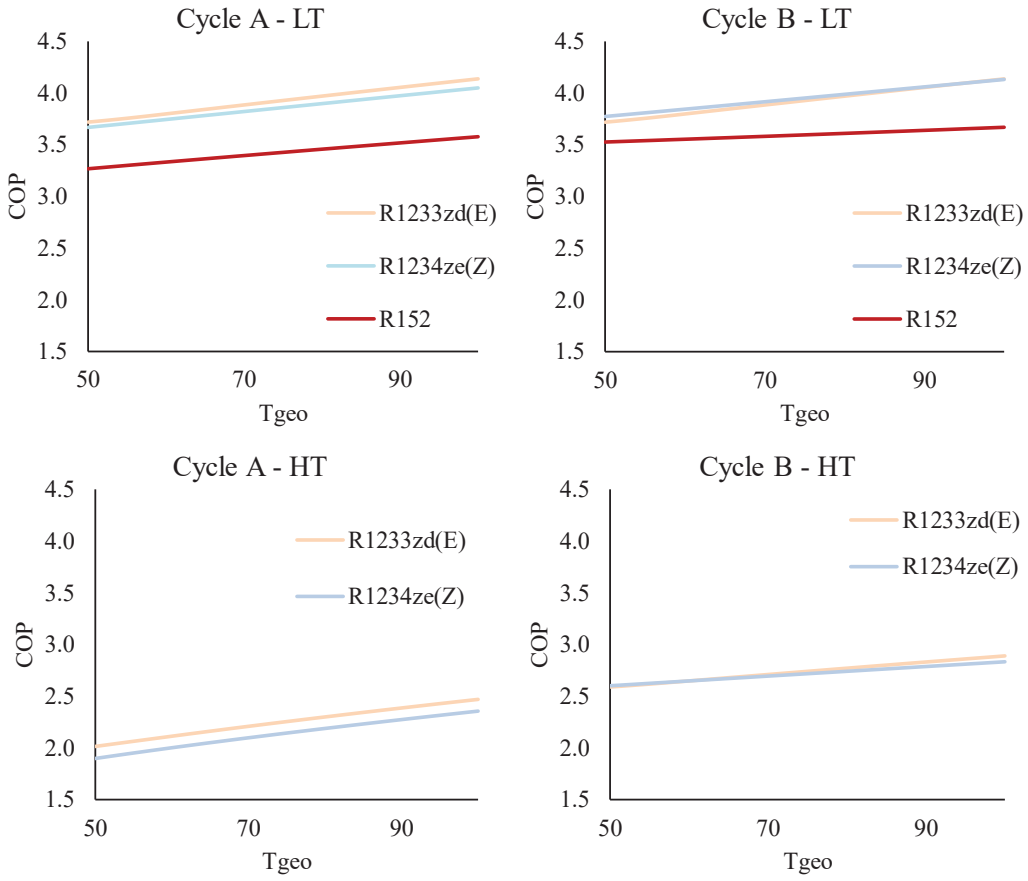

Figure 4: Graphs of the coefficient of performance (COP) of the different cycle cases: Top left Cycle A - Low temperature (LT) T_{cond} = 105°C, Top right Cycle B - LT, Bottom left Cycle A - High temperature (HT) T_{cond} = 140°C, Bottom right Cycle B - HT

https://doi.org/10.52202/077185-0136

4.2 General results of Metamodels: Economic, Environmental

The thermo-economic evaluation reveals significant variability in the Levelized Cost of Heat (LCOH) depending on resource conditions and well characteristics. Figure 5 shows LCOH, with 5a representing $well_{1000}$, 5b representing $well_{500}$, and 5c representing $well_{00}$. Additionally, the red dashed line represents the reference LCOH value provided by IEA 2021 for heat generated from natural gas-fired boilers, hovering around 17 c$/kWh, while the cost obtained for High-Temperature Heat Pumps (HTHP) is indicated as 22 c$/kWh (Jeßberger, J et al. 2023). It is evident that there is a substantial decrease in LCOH from 5a to 5c, highlighting the significant influence of drilling costs on this parameter. In 5a, it is observed that LCOH is exceedingly high for low value of T_{geo} and m_{geo}, reaching a maximum of 155 c$/kWh, with economic feasibility only apparent at higher temperatures or increased mass flow rates. In 5b, where the well depth is shallower, the maximum LCOH reduces to 100 c$/kWh, and more combinations of T_{geo} and m_{geo} surpass the red dashed line. Finally, in 5c, only a narrow range fails to yield an economic advantage, in fact, for all combinations of T_{geo}-m_{geo} above 62° C or above 17 kg/s, an LCOH below the boiler heat output is obtained. This underlines the dependence of LCOH on the cost of wells, which strongly affects the parameter. Therefore, for HTHP applications, cases where the geothermal reservoir is superficial, hot waste fluids from geothermal power plants or other situations without drilling wells would offer significant economic benefits. However, if a greater number of wells or deeper drilling is necessary, the conditions for LCOH advantage diminish considerably. Therefore, a careful evaluation is needed for each specific case according to the depth of the resource. The same areas assessed for the LT case are not displayed due to the consistent trend, with LCOH range variation being minimal, around 1-2 c$/kWh.

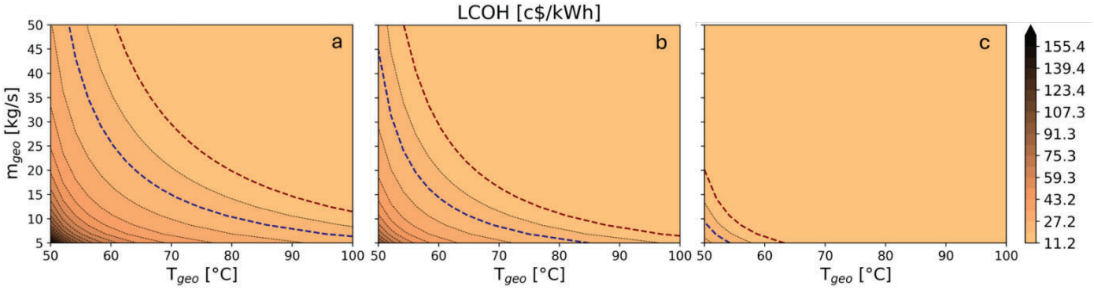

Figure 5: Techno-economic metamodel of the LCOH parameter for the three well depth scenarios: 5a $well_{1000}$, 5b $well_{500}$, 5c $well_{00}$

Figure 6 shows the metamodel of CC, equivalently for Figure 5. The environmental impact from geothermal HTHP has been much less studied in the literature so the limits are shown, a red one representing the CC indicator for a kWh produced by a natural gas modulating condensing boiler 264.16 g CO2 eq/kWh and the blue line for a kWh from a borehole heat exchanger brine-water 223.88 g CO2 eq/kWh evaluated by Ecoinvent providers. As can be seen, the trend is similar to the LCOH, where CC has a higher impact for case 6a whereas for low m_{geo} and T_{geo} 278 gCO2 eq/kWh which compared to normal boiler emissions is very similar. For this reason, temperatures above 60°C or m_{geo} above 15 kg/s are preferred to have a low environmental impact compared to other low-impact systems. It should be considered that, even in this case, the impact from drilling has a major contribution even if it is less incidental compared to the effect in LCOH, this is because CC also has a strong contribution from electricity production. As shown in both figures 6b and 6c, the potential for achieving low environmental impact is even greater, confirmed by a decrease in equivalent emissions. The borehole heat exchanger brine-water limits given in figure 6b only cover a small range for temperatures below 55° C. On the other hand, from figure 6c all cases are environmentally advantageous. Combining the information derived from both LCOH and CC, it appears that the limiting factor prevailing is the economic aspect rather than the environmental one. Therefore, for a comprehensive assessment of HTHP installation, priority should be given to economic viability over environmental considerations. The optimal conditions, as defined by economic metamodels, should guide decision-making processes in ensuring the most advantageous outcomes.

https://doi.org/10.52202/077185-0136

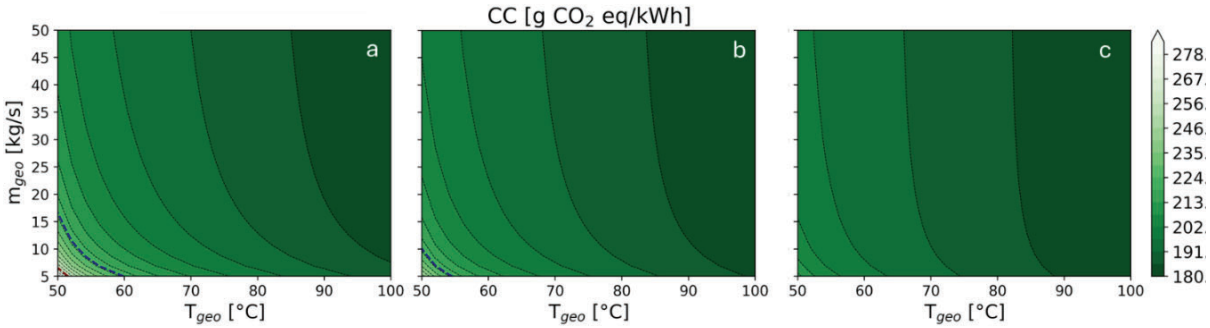

Figure 6: Figure 5: Environmental metamodel of the CC parameter for the three well depth scenarios: 5a $well_{1000}$, 5b $well_{500}$, 5c $well_{00}$

4.3 Results of Malawi case studies

Figure 7 shows the thermal energy produced by cycle B with R1234ze(Z) fluid, the corresponding LCOH and CC. The dashed red lines represent the heat demand for the three scenarios CS5k, CS10k, CS50k. The graph shows that in the case where m_{geo} is Lm for all wells, it is possible to satisfy the heat demand for a community of 5 thousand people CS_{5k}. A community of 10 thousand people CS_{10k} can be satisfied for some wells even in the case of Lm (Mtondolo 2, Chiwe, Mphizi stream). For all other wells, it is possible to satisfy this demand only in the case of Mm. The heat load of the CS_{50k} scenario is only reached for some sites in the Hm case (Chombo, Chiwe, Motombolo, Motombolo2 and Mphizi stream). It can also be noted that the two Madzimawira and Chiweta sites where the flow rates are known can meet the CS10k and CS50k heat loads respectively.

All scenarios have an LCOH that varies between 11.2 c$/kWh and 12.5 c$/kWh and are therefore very cost-effective. It is mainly due to the surface heat source, which allows for an extremely low LCOH. As far as CC is concerned, a larger variation is found, ranging between 197-186 gCO2/kWh. It is found that for wells with low T_{geo}, CC increases, and this is the result of the cycle behavior. In fact, the lower T_{geo} implies a larger difference between the low and high pressure of the cycle, which is reflected in a higher consumption of electricity by the compressor and thus a greater environmental impact.

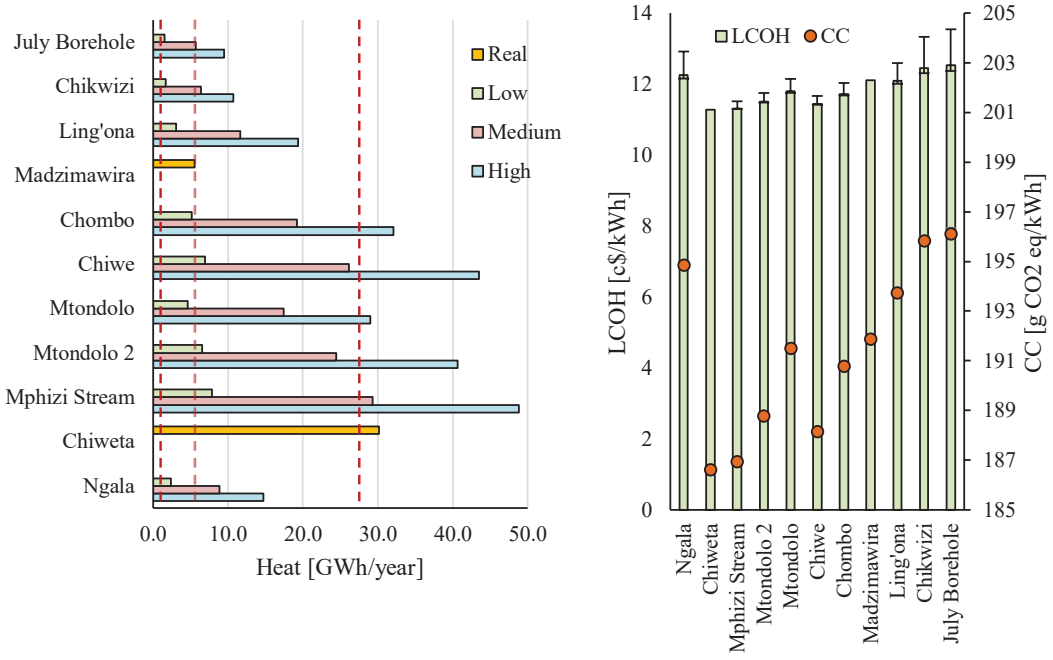

Figure 7: heat produced by cycle B with R1234ze(Z) fluid and corresponding LCOH and CC, for cooking station

https://doi.org/10.52202/077185-0136

For the Cassava drying application in Figure 8, it is shown that all wells even for Lm are able to meet the heat demand for drying of 10 k ton/year CD_{10}. As for the CD_{50} intermediate scenario, it is achieved with five wells in the case of Mm (Chombo, Chiwe, Motondolo, Motondolo 2 and Mphizi Stream).

In the Hm scenario, only three wells could reach the CD_{100} production level. For the Madzimawira and Chiweta cases, they can meet more than the heat demand of the CD_{10} and CD_{50} cases respectively. LCOH is for all scenarios between 6.8 - 8 c$ /kWh, therefore an extremely low value leading to strong cost-effectiveness. The LCOH variation from Lm and Hm is between 1 - 6 % for all scenarios excluding Chikwizi and July Borehole, which have a variation in the order of 10 %.

For CC it again turns out to be more variable, in the range of 130 to 139 gCO2/kWh which is far below the limits observed in the previous section.

The considerations done for the previous figure can be extended here as well, since the higher T_{geo} allows a reduction in environmental impact by reducing electrical energy consumption.

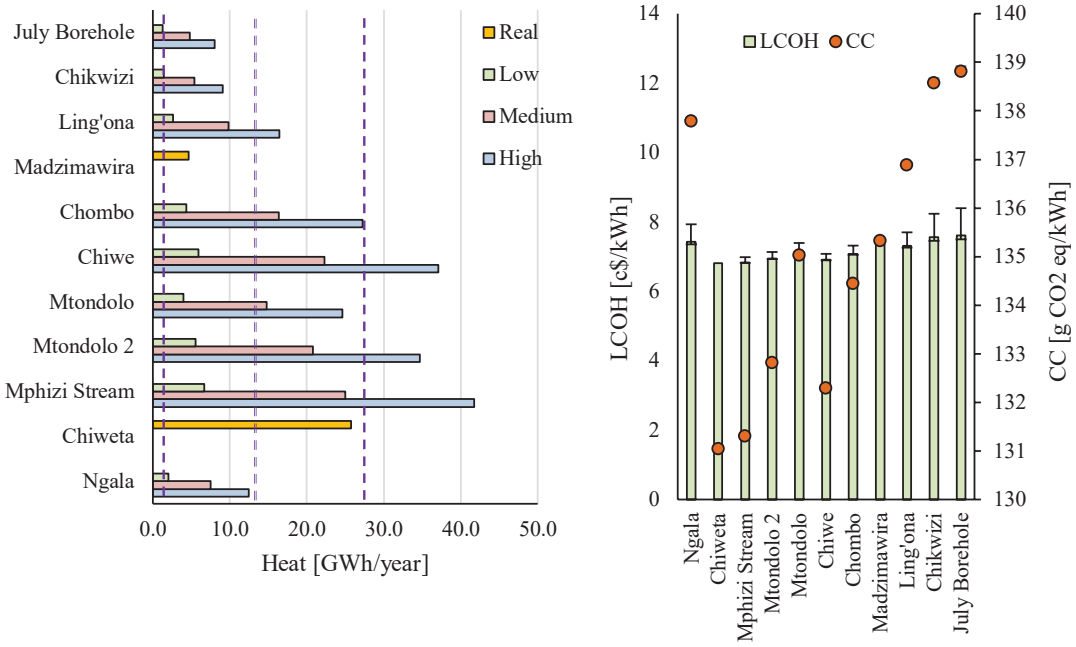

Figure 8: heat produced by cycle A with R1234ze(Z) fluid and corresponding LCOH and CC, for Cassava drying.

5 CONCLUSION

A comprehensive model capable of predicting the thermodynamic efficiencies, LCOH and environmental impacts associated with HTHPs coupled to geothermal energy sources has been realized and applied to an African case study. The analysis demonstrates the significant impact of drilling costs on LCOH, with deeper wells typically requiring higher investment. For instance, in scenarios with shallow wells, the LCOH can be as low as 6.8 - 8 c$/kWh, indicating strong cost-effectiveness. However, deeper drilling may lead to LCOH values exceeding 100 c$/kWh, necessitating careful consideration of well characteristics in economic assessments. Moreover, from an environmental point of view the analysis indicates that HTHP systems generally result in lower CC compared to conventional heating methods, particularly in scenarios with higher temperatures and optimized energy consumption. The analyses conducted reveals a significant potential in the utilization of high-temperature geothermal systems for various applications, including meeting the heat demand for cooking stations of different sizes and cassava drying. It has been demonstrated that even under the most unfavorable conditions, geothermal systems can achieve high levels of thermal efficiency, with

https://doi.org/10.52202/077185-0136

operating costs and environmental impacts significantly reduced compared to other conventional energy sources. Furthermore, the results indicate that the potential for greenhouse gas emissions reduction is largely influenced by the temperature of the geothermal fluid, which in turn reduces the electricity consumption associated with high-temperature heat pump cycles. Another way to further reduce this consumption is to exploit electricity from renewable sources, such as geothermal energy itself.
However, it is acknowledged that the decision to implement such systems should be guided not only by their economic efficiency but also by their overall environmental impact. Therefore, careful evaluation of both aspects is recommended to guide decisions regarding the selection and design of geothermal systems. In conclusion, the comprehensive evaluation of thermodynamic, economic and environmental factors underlines the potential of high temperature heat pump systems as a sustainable solution for various heating applications. The results suggest a multidisciplinary approach that balances economic considerations with environmental sustainability to maximize the benefits of HTHP technology in real-world implementations.

Reference

Budiarto, R., Indarto, S. H., & Sutrisno, S. (2014). Recent Development of Non-Conventional Geothermal Powerplant. Proceedings of the 3rd Applied Science for Technology Innovation; Aug, 13-14.

Cao, X. Q., Yang, W. W., Zhou, F., & He, Y. L. (2014). Performance analysis of different high-temperature heat pump systems for low-grade waste heat recovery. Applied thermal engineering, 71(1), 291-300. https://doi.org/10.1016/j.applthermaleng.2014.06.049

Chandrasekharam, D., & Bundschuh, J. (2008). Low-enthalpy geothermal resources for power generation. CRC press.

Dávalos-Elizondo, E., Atekwana, E. A., Atekwana, E. A., Tsokonombwe, G., & Laó-Dávila, D. A. (2021). Medium to low enthalpy geothermal reservoirs estimated from geothermometry and mixing models of hot springs along the Malawi Rift Zone. Geothermics, 89, 101963. https://doi.org/10.1016/j.geothermics.2020.101963

de Simón-Martín, M., Bracco, S., Piazza, G., Pagnini, L. C., González-Martínez, A., & Delfino, F. (2022). Levelized Cost of Energy in Sustainable Energy Communities: A Systematic Approach for Multi-Vector Energy Systems. Springer Nature. https://doi.org/10.1007/978-3-030-95932-6

Elbarbary, S., Zaher, M. A., Saibi, H., Fowler, A. R., Ravat, D., & Marzouk, H. (2022). Thermal structure of the African continent based on magnetic data: Future geothermal renewable energy explorations in Africa. Renewable and Sustainable Energy Reviews, 158, 112088. https://doi.org/10.1016/j.rser.2022.112088

Enerdata. Global energy statistical yearbook. 2013. Enerdata, Grenoble, France. (2013). Available at: http://www.enerdata.net/enerdatauk/press-and-publica-tion/ publications/world-energy-statistics-supply-and-demand.php.

Energy Regulatory Commission (ERC). (2012). Geothermal Resources, Renewable Energy Portal. Nairobi, Kenya: ERC

Energy Statistical Yearbook (ESY). Enerdata's free online interactive data tool. (2019). Available at: https://yearbook.enerdata.net/electricity/electricity-domestic-cons umption-data.html

IEA, Levelized cost of heating (LCOH) for consumers, for selected space and water heating technologies and countries, (2021) International Energy Agency, Paris https://www.iea.org/data-and-statistics/charts/levelized-cost-of-heating-lcoh-for-consumers-for-selected-space-and-water-heating-technologies-and-countries, IEA. Licence: CC BY 4.0

International Organization for Standardization (ISO), "ISO 14040:2021—Environmental management — Life cycle assessment — Principles and framework. Environ. Manage.," Geneva, Switzerland, 2021a.

International Organization for Standardization (ISO), "ISO 14044:2021 Environmental management - Life cycle assessment - Requirements and guidelines. Environ. Manage.," Geneva, Switzerland, 2021b.

Jeßberger, J., Heberle, F., & Brüggemann, D. (2023) Integration of high-temperature heat pumps into geothermal energy systems. *Gas*, *40*, 100.

Jin, H., Gao, L., Han, W., Li, B., & Feng, Z. (2007). Integrated energy systems based on cascade utilization of energy. Frontiers of Energy and Power Engineering in China, 1, 16-31. DOI 10.1007/s11708-007-0003-0

 https://doi.org/10.52202/077185-0136

Kajumba, P. K., Okello, D., Nyeinga, K., & Nydal, O. J. (2022). Assessment of the energy needs for cooking local food in Uganda: A strategy for sizing thermal energy storage with cooker system. Energy for Sustainable Development, 67, 67-80. https://doi.org/10.1016/j.esd.2022.01.005

Karimi, S., & Mansouri, S. (2018). A comparative profitability study of geothermal electricity production in developed and developing countries: Exergoeconomic analysis and optimization of different ORC configurations. Renewable Energy, 115, 600-619. https://doi.org/10.1016/j.renene.2017.08.098

Karlsdóttir, M. R., Pálsson, Ó. P., Pálsson, H., & Maya-Drysdale, L. (2015). Life cycle inventory of a flash geothermal combined heat and power plant located in Iceland. The International Journal of Life Cycle Assessment, 20, 503-519. https://doi.org/10.1007/s11367-014-0842-y

Kenya Ministry of Energy (KME). (2018). Geothermal. Nairobi, Kenya. Retrieved May 5th 2018 From http://energy.go.ke/geothermal/

Long-Termo Joint European Union-African Union Research and Innovation Partnership on Renewable Energy, Geothermal Atlas for Africa, LEAP-RE.GAA (2020). https://www.leap-re.eu/geothermal-atlas-4-africa/

Lund, J. W., Freeston, D. H., & Boyd, T. L. (2011). Direct utilization of geothermal energy 2010 worldwide review. Geothermics, 40(3), 159-180. https://doi.org/10.1016/j.geothermics.2011.07.004

Lund, J. W., & Boyd, T. L. (2016). Direct utilization of geothermal energy 2015 worldwide review. Geothermics, 60, 66-93. https://doi.org/10.1016/j.geothermics.2015.11.004

Mosaffa, A. H., Farshi, L. G., Ferreira, C. I., & Rosen, M. A. (2016). Exergoeconomic and environmental analyses of CO2/NH3 cascade refrigeration systems equipped with different types of flash tank intercoolers. *Energy Conversion and Management*, *117*, 442-453. https://doi.org/10.1016/j.enconman.2016.03.053

Mosaffa, A. H., Mokarram, N. H., & Farshi, L. G. (2017). Thermoeconomic analysis of a new combination of ammonia/water power generation cycle with GT-MHR cycle and LNG cryogenic exergy. Applied Thermal Engineering, 124, 1343-1353. https://doi.org/10.1016/j.applthermaleng.2017.06.126

Nwakuba, N. R., Asoegwu, S. N., & Nwaigwe, K. N. (2016). Energy requirements for drying of sliced agricultural products: a review. Agricultural Engineering International: CIGR Journal, 18(2), 144-155.

Rubio-Maya, C., Díaz, V. A., Martínez, E. P., & Belman-Flores, J. M. (2015). Cascade utilization of low and medium enthalpy geothermal resources− A review. Renewable and Sustainable Energy Reviews, 52, 689-716. https://doi.org/10.1016/j.rser.2015.07.162

Shamoushaki, M., Fiaschi, D., Manfrida, G., Niknam, P. H., & Talluri, L. (2021). Feasibility study and economic analysis of geothermal well drilling. International Journal of Environmental Studies, 78(6), 1022-1036. https://doi.org/10.1080/00207233.2021.1905309

Shamoushaki, M., Fiaschi, D., Manfrida, G., & Talluri, L. (2022). Energy, exergy, economic and environmental (4E) analyses of a geothermal power plant with NCGs reinjection. Energy, 244, 122678. https://doi.org/10.1016/j.energy.2021.122678

Stober, I., & Bucher, K. (2013). Geothermal energy. Germany: Springer-Verlag Berlin Heidelberg. doi, 10, 978-3. https://doi.org/10.1007/978-3-030-71685-1

TRANE, Exergy, (2022). Industrial Heat Pump. Report-Catalogue. https://trane.eu/it/equipment/2-heat-pumps.html

Turton, R., Bailie, R. C., Whiting, W. B., & Shaeiwitz, J. A. (2008). *Analysis, synthesis and design of chemical processes*. Pearson Education.

Waruru, M. (2016). Kenya on Track to More Than Double Geothermal Power Production. Renewable Energy World. Retrieved from: http://www. renewableenergyworld. com/articles/2016/06/kenya-on-track-to-more-than-doublegeothermal-power-production. html.

Zuffi, C., Manfrida, G., Asdrubali, F., & Talluri, L. (2022). Life cycle assessment of geothermal power plants: A comparison with other energy conversion technologies. Geothermics, 104, 102434. https://doi.org/10.1016/j.geothermics.2022.102434

https://doi.org/10.52202/077185-0136